



Analytical Discernment of Electromagnetically Induced Transparency from Autler-Townes Splitting for Atom Based E-field Sensing

Satya Kesh Dubey*

CSIR-National Physical Laboratory, New Delhi, Delhi, India

Abstract

In this work, the Density Matrix equations of motion for a four-level ladder ^{85}Rb atomic model has been analyzed analytically to gain the physical intuition behind the similar looking interference phenomena like Electromagnetically Induced Transparency (EIT) and Autler-Townes Splitting (ATS). This work gives the theoretical insight of the new atomic-transitions based technique for Radio-Frequency (RF) E-field strength measurement which may get accepted internationally as a new standard for accurate and precise measurements of E-field as it is dependent only on physical constants and is directly traceable to SI units. The potential sources of ambiguity and uncertainty in the experiment has been discussed. Interestingly, we observed that ATS can also be achieved in EIT regime.

1. Introduction

At present, there is a constant motivation across the globe in all the metrology laboratories to make all the measurements traceable to the basic SI units or some physical universal constants. By doing so, one can perform the measurements with the confidence of the fidelity in the observations. For the confidence in measurements the classical metrology practices under use till now prove to be more challenging. The dependency on the materials under use, the surrounding parameters at the time of measurement, and the incorrect evaluation of uncertainties are some of the limitations of current techniques which makes measurable quantity vulnerable to the errors not tolerable in today's science. Quantum metrology techniques are promising as they offer self-calibrating characteristics for the measured quantities with dependency only on the physical constants instead of temperature, humidity, material under use etc.

In the field of electromagnetic measurements, the accuracy in the measurement of E-field amplitude plays a crucial role in the determination of many other parameters such as Specific Absorption Rate (SAR) in biomedical application, EMI/EMC testing of RF and electronic devices, non-invasive RF based detection and diagnostic medical devices, etc. With the rise in the need for precise and accurate measurement of E-field amplitude, arises the

need for the new technique to realize the amplitude flawlessly. The lack of traceability in the RF E-field strength measurements has been a major source of errors throughout the years and limits the growth of research works requiring impeccable measurements. Moreover, till now we don't have the E-field sensors which work in the Infrared region clearly showing the measurable gap in the electromagnetic spectrum. Atom-based metrology standards have been widely accepted in the recent past for a number of measurements namely length, time, and frequency [1, 2]. This approach facilitates the stated goal of direct SI traceability in the measurements.

The present calibration process of the E-field probes poses indirect and complex traceability path thus making it a very challenging task to perform. To calibrate them one need a known field in the testing room and to ensure the field in the room one again need a probe to read it. To overcome this dilemma during the calibration process, research work is going on to realize the RF E-field strength measurement through the atomic transitions based approach discussed here [1 - 5].

This novel technique is based on the interaction of the highly excited alkali atoms with RF energy and utilizes the concepts of quantum interference phenomena like EIT and ATS. Under this technique, a cell containing vapors of alkali atoms is a possible candidate for a broadband probe scanning from RF to Infrared region. The present E-field probes can sense the E-field strength of approximately 100mV/m, but with the atom-based quantum E-field metrology technique the probe can sense as low as $1 \mu\text{V/m}$ of field strength with sensitivity of $1 \mu\text{V m}^{-1} \text{ Hz}^{-1/2}$ [1]. Moreover, this technique may be used to sense and measure the frequencies up to the terahertz range. Before carrying out experimental observations one should conceive a thorough physical understanding, and should be able to distinguish between the two similar looking phenomena with ease.

EIT can be observed in three level systems also with two resonant coupling fields providing different pathways for resonances giving rise to the destructive interference and hence dip in the probe absorption [6, 7]. It is also well known that strong driving field can modify the characteristics by changing the transitions resulting in

doublet spitting of absorption and is interpreted as dynamic Stark-splitting [8] similar to the Autler-Townes Splitting [9].

2. Atomic Model and Equations of Motion

To explore the probe absorption through a medium, an atomic vapor cell of ^{85}Rb under the simultaneous influence of two optical fields and one RF field is considered for this work; the laser configuration consisting of two lasers in counter-propagating direction is depicted in figure 1(a). Figure 1(b) shows the 4-level ladder atomic model under consideration with the weak red laser (780nm) probing the atomic ensemble for the response and will be referred to as ‘probe’ throughout this work. Probe with Rabi frequency $2\Omega_p$ is tuned to D_2 line of ^{85}Rb and couples ground state $5S_{1/2}$ to $5P_{3/2}$. Another optical field, strong laser (480nm) with Rabi frequency $2\Omega_c$ pumped the atom into the excited Rydberg state (couples states $5P_{3/2}$ and $5D_{5/2}$) and will be referred to as ‘pump’ hereafter.

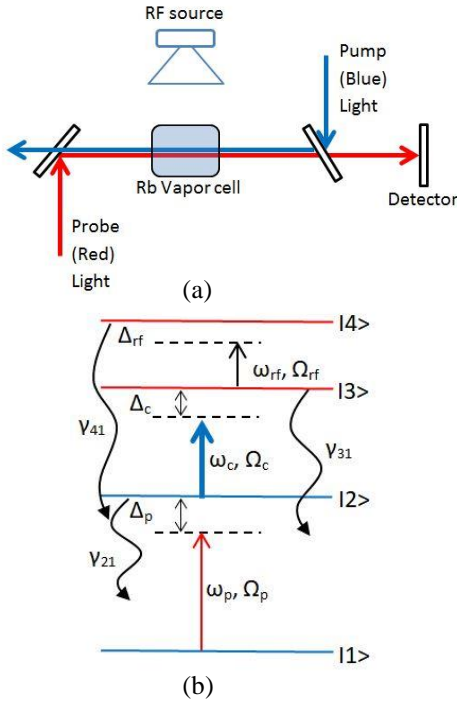


Figure 1. (a) Representational setup for the atomic transitions based E-field metrology; (b) Energy level structure of the atom.

RF energy cannot cause any transitions in the ground states of ^{85}Rb as it needs high energy with a frequency in the range of typical optical region to excite the Rb atom from ground state to excited state. If the atom is highly excited, then the amount of energy required for atomic transitions would be very less and can be achieved easily through RF energy, in our case RF couples Rydberg states $5D_{5/2}$ and $5F_{7/2}$ represented by |3> and |4> shown in red in fig. 1(b).

The evolution of the system with time can be determined by writing the equations of motion in the interaction picture and under rotating-wave approximation and can be written as

$$i\dot{\rho}_{11} = i\Gamma_{12}\rho_{22} - \Omega_p\rho_{12} + \Omega_c^*\rho_{21} \quad (1)$$

$$i\dot{\rho}_{22} = i\Gamma_{23}\rho_{33} - i\Gamma_{12}\rho_{22} - \Omega_c\rho_{23} + \Omega_c^*\rho_{32} + \Omega_p\rho_{12} - \Omega_p^*\rho_{21} \quad (2)$$

$$i\dot{\rho}_{33} = i\Gamma_{23}\rho_{33} - i\Gamma_{23}\rho_{33} - \Omega_{rf}\rho_{34} + \Omega_{rf}^*\rho_{43} + \Omega_c\rho_{23} - \Omega_c^*\rho_{32} \quad (3)$$

$$i\dot{\rho}_{44} = -i\Gamma_{34}\rho_{44} - \Omega_{rf}\rho_{34} - \Omega_{rf}^*\rho_{43} \quad (4)$$

$$i\dot{\rho}_{21} = t_2\rho_{21} + \Omega_p(\rho_{22} - \rho_{11}) + \Omega_c\rho_{31} \quad (5)$$

$$i\dot{\rho}_{31} = t_3\rho_{31} + \Omega_{rf}\rho_{41} + \Omega_c\rho_{21} - \Omega_p^*\rho_{32} \quad (6)$$

$$i\dot{\rho}_{41} = t_4\rho_{41} + \Omega_{rf}\rho_{31} - \Omega_p^*\rho_{42} \quad (7)$$

$$i\dot{\rho}_{32} = (\Delta_c - i\gamma_{23})\rho_{32} + \Omega_c(\rho_{33} - \rho_{22}) + \Omega_{rf}\rho_{43} - \Omega_p^*\rho_{31} \quad (8)$$

$$i\dot{\rho}_{43} = (\Delta_{rf} - i\gamma_{34})\rho_{43} + \Omega_{rf}(\rho_{44} - \rho_{33}) - \Omega_c^*\rho_{42} \quad (9)$$

where the parameters t_2, t_3 and t_4 are complex detunings and are given by, $(\Delta_p - i\gamma_{21})$, $(\Delta_p + \Delta_c - i\gamma_{31})$, $(\Delta_p + \Delta_c + \Delta_{rf} - i\gamma_{41})$ respectively. With detunings $\Delta_p = \omega_p - \omega_{12}$, $\Delta_c = \omega_c - \omega_{23}$, $\Delta_{rf} = \omega_{rf} - \omega_{34}$ with ω_{ij} the on-resonance angular frequency for the state i to j transition, and spontaneous decay rates (γ_{ij}) and relaxation rates (Γ_{ji}) from the upper state i to lower state j .

Solving this set of equations by applying the weak probe conditions, the off-diagonal element corresponding to the probe transition can be obtained as

$$\rho_{21} = \Omega_p \frac{(\Omega_{rf}^2 - t_3 t_4)}{\Omega_{rf}^2 t_2 - t_2 t_3 t_4 + \Omega_c^2 t_4} \quad (10)$$

Utilizing the above expression, the RF E-field strength can be determined by measuring the separation between the two peaks in the probe absorption spectrum and is given by

$$E_{rf} = 2\pi\Delta f \frac{\hbar}{d_{rf}} \quad (11)$$

where \hbar is the Planck's constant, d_{rf} is the atomic dipole moment of RF transition and can be evaluated by utilizing the quantum defects of ^{85}Rb [10]. Δf is the splitting in the absorption peak, thus converting the amplitude

measurement of RF E-field into frequency measurement which can be measured very accurately.

3. Results and Discussions

Figure 2 shows the response of probe transmission signal with respect to the probe detuning through the vapor cell in the presence of different values for RF Rabi frequency. The results shown in this figure are similar to the results obtained by C. L. Holloway *et.al.* in ref. [3]. Other parameters are kept same as were in [3], *i.e.* $\gamma_{12} = 2\pi 6.066$ MHz, $\gamma_{13} = \gamma_{14} = 10^{-4} \gamma_{12}$ MHz. Here we take the coupling laser frequency and RF frequency to be resonant in their respective transitions *i.e.* $\Delta_c = \Delta_{rf} = 0$.

The red curve corresponds to the situation when $\Omega_c = 0$ and $\Omega_{rf} = 0$. It clearly represents the full absorption of the probe signal with no sign of EIT in the medium. Green curve is for $\Omega_{rf} = 0$, and $\Omega_c = 40$ MHz, in this case split in the absorption has been observed and is referred to as an EIT, with zero absorption at the center of the transparent window. Further, when keeping pump fixed and RF Rabi frequency is changed the transparent window further splits into two and the difference between two peaks increases with increase in the RF Rabi frequency, shown by the orange and blue curves. This change in the EIT signal in presence of RF energy is referred to as ATS splitting of the EIT peak.

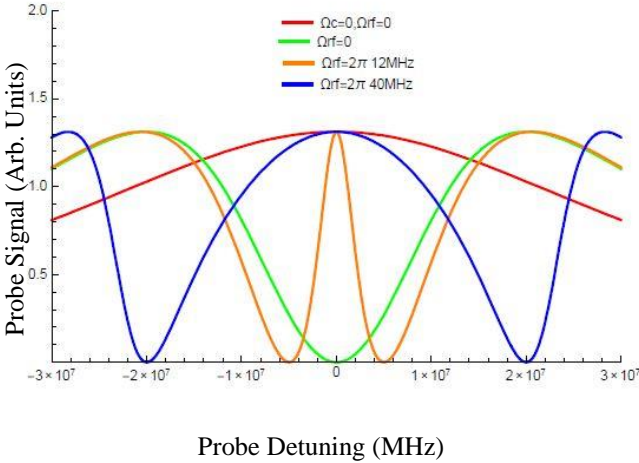


Figure 2. Probe absorption versus probe detuning (Δ_p) for different values of RF Rabi frequency. This graph is reproduced from C. L. Holloway *et.al.* [3].

Figure 3 represents the case when spontaneous decay rates between the states are changed by keeping all the parameters same as were in the case of figure 2, and the results are worth noticing. In this case, decay rates are $\gamma_{12} = 1$ MHz, $\gamma_{14} = 3$ MHz, and $\gamma_{13} = 0$ MHz. The change in the behavior of probe signal can be seen very conveniently, as the pump Rabi frequency increases the amplitude of the transmission signal decreases, this may be the case when the ATS effect becomes dominant as mentioned in reference [4].

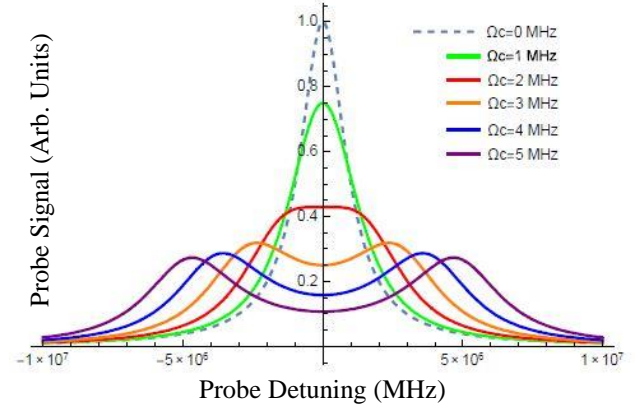


Figure 3. Probe absorption versus probe detuning (Δ_p) for different values of pump Rabi frequency.

Next, we show the effect of RF energy on the probe transmission as a function of probe detuning by keeping Rabi frequency of probe and pump fixed. Figure 4 shows the probe signal in presence of RF field. Ω_c is kept as 15 MHz and all the parameters are same as in figure 3. We observed that in 4-level cascade atomic model RF energy provides the pathways within the degenerate Rydberg states for constructive interference in the continuum, giving rise to the third peak in middle of the transparent window, which is, in this case we believe is dynamic stark shift or Autler-Townes Splitting in the EIT regime.

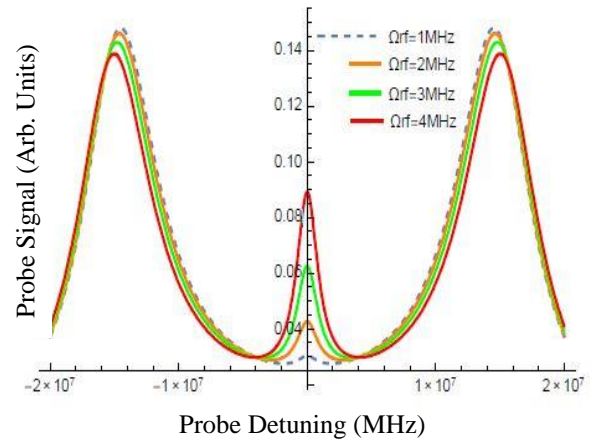


Figure 4. Probe absorption versus probe detuning (Δ_p) for different values of RF Rabi frequency.

It can be seen in the plots shown in ref. [4] that when RF is turned ON there is a significant rise in the third peak in the center of the transparent window which we believe is because of the constructive interference in the continuum due to RF source. For the fixed probe and pump frequency a time will come when the third peak will be dominant and the splitting cannot be measured easily, in this case again the probe and pump frequencies will be scanned for same frequency and E-field amplitude of radio-frequency source. In this manner, number of

combinations can be obtained for the measurement of E-field of RF over a wide range of frequencies.

The sources of uncertainties in the experiment are currently under study. Some of the possible sources of uncertainties in this method are: (1) The walls of vapor cell are generally made up of Quartz or Pyrex which can reflect or absorb the E-field. (2) Standing waves can also be formed inside the cell because of reflections, which can be a further source of uncertainty as the E-field inside the cell will be different. (3) The evaluation of dipole moment of RF transition can deviate from the true value. (4) The evaluation of atom number density inside the vapor cell may vary.

4. References

1. H. Fan, S. Kumar, J. Sedlacek, H. Kübler, S. Karimkashi, & J. P. Shaffer, "Atom based RF electric field sensing," *Journal of Physics B: Atomic, Molecular and Optical Physics*, 48, 20, September 2015, p. 16, doi: 10.1088/0953-4075/48/20/202001.
2. C. L. Holloway, M. T. Simons, J. A. Gordon, P. F. Wilson, C. M. Cooke, D. A. Anderson, and G. Raithel, "Atom-Based RF Electric Field Metrology: From Self-Calibrated Measurements to Subwavelength and Near-Field Imaging," *IEEE Transactions on Electromagnetic Compatibility*, 59, 2, January 2017, pp. 717-728, doi: 10.1109/TEMC.2016.2644616.
3. C. L. Holloway, J. A. Gordon, S. Jefferts, A. Schwarzkopf, D. A. Anderson, S. A. Miller, N. Thaicharoen, and G. Raithel, "Broadband Rydberg Atom-Based Electric-Field Probe for SI-Tracable, Self-Calibrated Measurements," *IEEE Transactions on Antennas and Propagation*, 62, 12, December 2014, pp. 6169-82, doi: 10.1109/TAP.2014.2360208.
4. C. L. Holloway, M. T. Simons, J. A. Gordon, A. Dienstfrey, D. A. Anderson, and G. Raithel, "Electric Field Metrology for SI Traceability: Systematic Measurement Uncertainties in Electromagnetically Induced Transparency in Atomic Vapor," *Journal of Applied Physics*, 121, 23, June 2017, pp. 9, doi: <https://doi.org/10.1063/1.4984201>.
5. J. A. Sedlacek, A. Schwettmann, H. Kubler, R. Low, T. Pfau, and J. P. Shaffer, "Microwave Electrometry with Rydberg Atoms in a Vapour Cell Using Bright Atomic Resonances," *Nature Physics*, 8, November 2012, pp. 819-24. Doi: 10.1038/NPHYS2423.
6. K. J. Boller, A. Imamoglu, and S. E. Harris, "Observation of electromagnetically induced transparency," *Physical Review Letters*, 66, 20, May 1991, pp. 2593-96, doi: <https://doi.org/10.1103/PhysRevLett.66.2593>
7. A. K. Mohapatra, T. R. Jackson, and C. S. Adams, "Coherent Optical Detection of Highly Excited Rydberg States Using Electromagnetically Induced Transparency," *Physical Review Letters*, 98, 113003, March 2007, pp. 1-4. doi: 10.1103/PhysRevLett.98.113003.
8. C. Wei, and N. B. Manson, "Observation of Dynamic Stark Effect on Electromagnetically Induced Transparency," *Physical Review A*, 60, 3, September 1999, pp. 2540-46 doi: <https://doi.org/10.1103/PhysRevA.60.2540>
9. S. H. Autler, and C. H. Townes, "Stark Effects in Rapidly Varying Fields," *Physical Rev.*, 100, 2, May 1955, pp. 703-722, doi: <https://doi.org/10.1103/PhysRev.100.703>.
10. I. I. Sobelman, *Atomic Spectra and Radiative Transitions*, 2nd. ed. (Springer 1996).